JOURNAL OF MATERIALS SCIENCE 25 (1990) 3133–3138

Thermal evaporation of tin on to softened polystyrene substrates

R. S. PAYNE, A. SWANN, P. J. MILLS
Department of Materials Science and Engineering, University of Surrey, Guildford, Surrey, GU2 5XH, UK

Transmission electron microscopy is used to investigate the tin deposits formed when tin is thermally evaporated on to softened polystyrene substrates, the polystyrenes being softened by heating them to above their glass transition temperature. The structure of the deposit is dependent on the molecular weight of the polystyrene. For low molecular weights, islands of tin grown on the polystyrene surface rapidly "sink" to form a microstructure consisting of sub-surface spheres of tin. As the molecular weight is increased the reduced rate at which islands can sink is reflected in the particle size distribution of the deposit.

1. Introduction

When a metal is thermally evaporated on to a polymeric substrate, then providing $\tau_1 > \tau_2 + \tau_{12}$ where τ_1, τ_2 and τ_{12} are the surface energies of the metal, polymer and interface, respectively, the formation of a sub-surface deposit of metal is thermodynamically favourable. However, using transmission electron microscopy (TEM) to determine the location of the deposit, Kovacs and Vincett [1] have shown that with a system of tin and a styrene-hexylmethacrylate copolymer, the growth of sub-surface deposits only occurs if the deposition is undertaken within a well-defined regime of deposition rate and substrate temperature, the substrate temperature having to be above the glass transition temperature (T_g) of the copolymer. The structure of the sub-surface deposit consisted of spheres of a narrow size distribution. The size could be controlled at constant packing density simply by controlling the quantity of tin deposited. In their experiments a typical diameter for the spheres produced was 0.1 μm. A schematic diagram that summarizes their results is shown in Fig. 1. At high temperatures and low deposition rates, where the adatom concentration is low, no nucleation of a deposit occurs. Of concern here, however, is the boundary between the regions of surface and subsurface deposit.

Fig. 1 has been used by Kovacs and Vincett [1] as support for a growth mechanism for the sub-surface deposit that involves the surface nucleation and growth of metal islands which then sink and coalesce beneath the surface. Firstly using theoretical considerations described by Robinson and Robins [2], the dotted boundary (B1), was shown to correspond to the transition in the growth of above-surface deposits from the required Volmer–Weber (island formation) mode to the Stranski–Krastinov (continuous layer formation) mode [3]. The sinking process was then modelled as described in the Appendix. In the model the islands are considered to be spheres, the major contribution to the driving force for sinking being the reduction in surface energy. If this force is opposed by a viscous drag given by Stokes' formula [4], then the volume flux (F), of metal through the polymer surface would be given by

$$F = (4\pi\tau_2 Na^2)/\{9\eta \ln [(\tau_1 + \tau_2 - \tau_{12})/ \times (\tau_1 - \tau_2 - \tau_{12})]\} \quad (1)$$

where a is the radius of the spherical islands, and N the number of islands per unit area and η the viscosity of the polymer.

To form their large particles of sub-surface deposit, Kovacs and Vincett suggested that the deposition flux (R), had to be less than F. The solid boundary (B2), in Fig. 1, would therefore define where F is equal to R. Kovacs and Vincett showed that the slope of B2 above T_g corresponded to an activation energy similar to that for viscous flow of the polymer. Moreover, by setting the areal coverage $N\pi a^2 = 0.6$, the value for randomly packed spheres (i.e. the maximum surface coverage possible that would not impose additional restrictions on sinking), their model accurately predicted its position.

While Kovacs and Vincett have shown these structures to form in softened substrates for a wide variety of systems [1, 5–8], the structures have also been observed when the polymer was beneath T_g [9]. In this case it would appear that the flux of metal through the polymer surface is by adatoms diffusing into the polymer. Nucleation would then occur beneath the surface and growth of the particles would be by capture of adatoms diffusing into the bulk. This mechanism of growth cannot be ruled out for softened substrates. Indeed one would anticipate a boundary between regions of surface and sub-surface particulate formation corresponding to $F = R$, similar to the solid boundary in Fig. 1, as the diffusion of the metal is, of course, also thermally activated.

The problem with varying deposition rate and substrate temperature in order to investigate the

0022–2461/90 $03.00 + .12 © *1990 Chapman and Hall Ltd.*

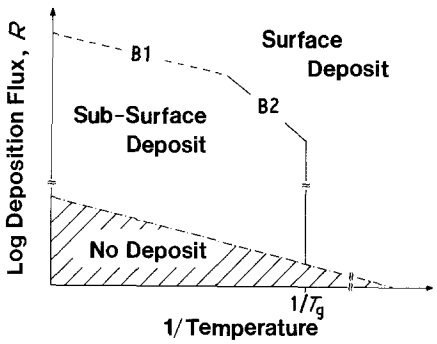

Figure 1 A schematic diagram summarizing the results of Kovacs and Vincett [1, 5–8].

formation of a sub-surface deposit, is that surface parameters such as the adatom concentration, and hence the kinetics of nucleation and growth of a surface deposit will also be varying.

In this paper we report the results from two series of experiments concerned with the formation of sub-surface deposits of tin in polystyrene (PS). They show that by varying the molecular weight (M) of the PS, insight into the mechanism and kinetics of formation of such deposits can be gained, while keeping deposition rate and substrate temperature constant.

In the first series of depositions (Series A, Table I), the molecular weight of an originally linear PS was increased by cross-linking using e^- beam radiation. In the second series of experiments (Series B, Table I) linear PS standards for a range of molecular weights were used.

2. Experimental details

Images of the deposits were obtained using a Phillips 400T TEM. Specimens were prepared by first casting ≈ 200 nm thick films from a toluene solution on to NaCl crystals. After deposition, the NaCl could be dissolved and the PS and deposit picked up on a microscope grid. The particle size distributions were averaged over at least five regions of the specimens using a Quantimet 920. To determine the location of the deposits cross-sections through the PS surface were prepared. For these specimens, thicker ($\approx 1\ \mu$m) PS films were used. To provide a "marker" of the PS surface, an additional deposition of gold with the PS at room temperature was undertaken. Deposition under these conditions is known to result in a surface layer of gold [10]. The sample was then embedded in mounting resin (Scandiplast 9101 Skye Instruments Ltd, Llandrjndeg) for microtomy. It should be noted that this resin is known not to plasticize or dissolve PS.

The deposition parameters are summarized in Table I. Depositions were undertaken with a background pressure of less than 10^{-6} torr. The nominal film thickness of the deposits and deposition rates were measured using a quartz crystal rate deposition monitor.

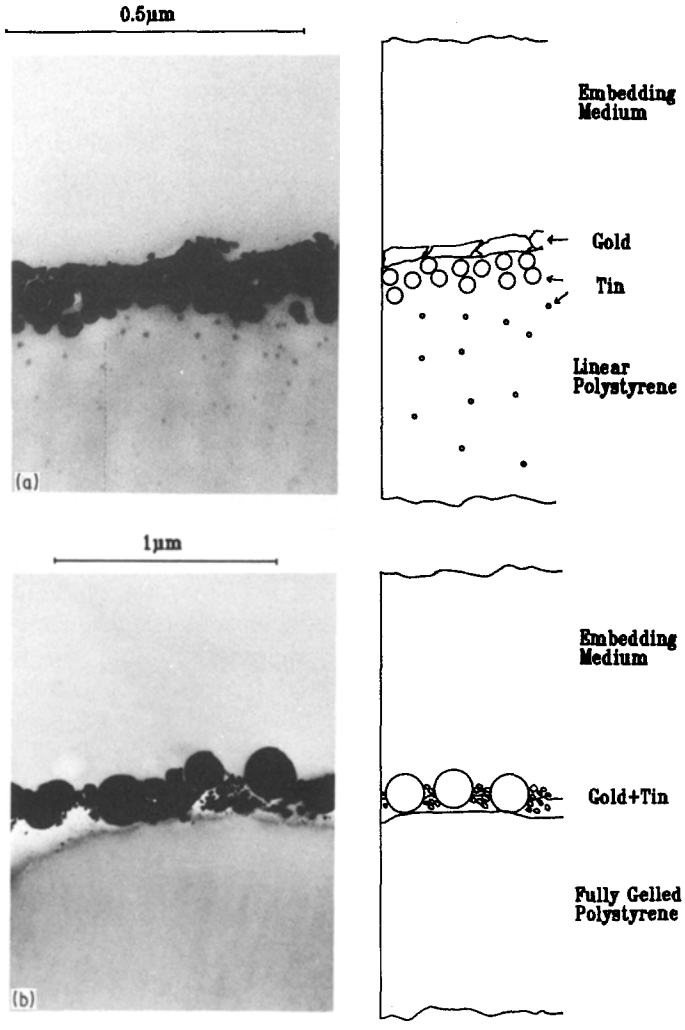

Figure 2 Series A. Cross-sectional transmission electron micrographs showing (a) sub-surface tin particles formed in PS, $M = 1.8 \times 10^6$, (b) surface particles formed on fully gelled PS, $M = 1.8 \times 10^6$, cross-linked to $10 \times D_{gel}$. (NB A small mount of gold deposited at room temperature was used to mark the specimen surface in each case.)

TABLE I Deposition parameters

Depositions	PS mol wt, M	Substrate Temp. (K)	Dep. rate ($nm\,sec^{-1}$)	Nominal film thickness (nm)
Series A	3.5×10^4, 1.8×10^6	493	0.1	35
Series B	3.5×10^4, 4×10^5, 1.8×10^6	473	0.1	15

In series A the cross-linking of the PS was undertaken using a 30 kV electron beam operating at a power density of $6 \times 10^{-5}\,W\,m^{-2}$. The background pressure during cross-linking was less than 10^{-6} torr. The cross-linking efficiency, G_x (the number of cross-links formed per 100 eV of energy adsorbed) was found by adopting the procedure of Charlesby and Pinner [11]. The sol fraction of the PS (obtained by measuring the weight loss of the irradiated PS after immersion in toluene) was measured as a function of dose in order to determine the dose for incipient gelation in the sample. At this "gel-dose", (D_{gel}), there is one cross-link per weight average molecule originally present. From the molecular weight of the polymer and the rate of energy loss of the electrons through the PS [12]), values of G_x were found for $M = 3.5 \times 10^4$ and 1.8×10^6. These values were equal to 0.070 ± 0.005; a result which is in good agreement with values reported by other authors [13, 14]. It should also be noted that X-ray photoelectron spectroscopy gave no indication of incorporation of oxygen in the PS surface during cross-linking.

3. Results and discussion

3.1. Series A

Fig. 2 shows micrographs of the cross-sections of the deposit formed with substrates of linear PS of $M = 1.8 \times 10^6$ and the same polymer radiated to $10 \times D_{gel}$. Given this dose the PS is completely gelled which would prevent island sinking. However, due to the high molecular weight of the initial polymer, the concentration of cross-links is still very low. Indeed, if one considers that the mean square end-to-end distance of a PS chain ($\bar{R}^2$) is given by [15]

$$\bar{R}^2 = 0.0049M \quad (nm^2)$$

then the distance between cross-links is approximately 30 nm. As this is so much larger than the dimensions of atomic tin, it seems reasonable to assume that the diffusion coefficient of atomic tin will be unaffected by the presence of cross-links.

Energy dispersive X-ray analysis (EDAX), was used to resolve the tin and the gold particles in the deposit. Deposition on the linear PS has resulted in a sub-surface deposit of tin spheres; the gold appearing as a near-continuous layer on the PS surface. However, for the cross-linked PS the tin spheres were larger and located on the surface of the PS. Small, irregular particles of gold can be seen between the tin spheres. Hence we have clear evidence to support a mechanism for the formation of sub-surface tin deposits in PS which involves island sinking.

The effect of cross-linking on the particle size distribution and the mean particle radius ($\bar{R}_p$) is shown in Fig. 3. This shows plan view micrographs of the deposits and the corresponding particle size distributions formed on substrates of linear PS of $M = 3.5 \times 10^4$, together with this same PS irradiated with $0.5 \times D_{gel}$ and $1.0 \times D_{gel}$. As the cross-link density is increased there is an increase in the range of particle sizes, and a transition from a monomodal to a bi-modal distribution. It should be noted that experiments were performed for cross-link doses above $1.0 \times D_{gel}$ but no significant differences in the particle size distributions from that displayed for $1.0 \times D_{gel}$ were observed.

To show that these trends are a result of the cross-links reducing the rate of island sinking in these softened substrates, an identical deposition was undertaken on a graphite substrate where no island sinking can occur. The resulting particle size distribution is also shown in Fig. 3. It is strikingly similar to that obtained on the PS irradiated to $1.0 \times D_{gel}$.

To explain the distributions we must consider stages during the growth by the Volmer–Weber mechanism of a deposit on a rigid substrate [3, 16].

Stage 1: adatoms that do not re-evaporate can, by diffusion about the surface, participate in the formation of stable nuclei.

Stage 2: the population of stable nuclei increases, but there is an increased probability that adatoms are "captured" by existing nuclei which then grow to form larger islands of deposit.

Stage 3: the density of islands become sufficiently large that all adatoms are captured by existing islands, i.e. no further nucleation occurs.

Stage 4: the islands become so large that they may coalesce [17, 18]. Coalescence results in free surface being generated, in which further nucleation can then occur.

Stage 5: islands grow into each other to form a continuous layer of deposit.

Clearly Stage 5 has not been reached in any of the depositions. However, a bi-modal particle size distribution is indicative of the concurrent nucleation and coalescence of stage 4. Indeed in Fig. 3, the smaller particles in the bi-modal distributions formed on the graphite and the PS irradiated to $1.0 \times D_{gel}$ can be seen in the near vicinity of the larger particles. The fact that this stage is not reached for the linear PS can be attributed to the surface concentration of islands being reduced by sinking. The kinetics of sinking will now be considered with the aid of the results from experimental series B.

3.2. Series B

A number of major assumptions were made in the model which led to the derivation of Equation 1 (these are outlined in the Appendix). However, as it has proven reasonably successful in describing the results of Kovacs and Vincett, it is worth considering what it predicts for this experimental series. Bulk values of

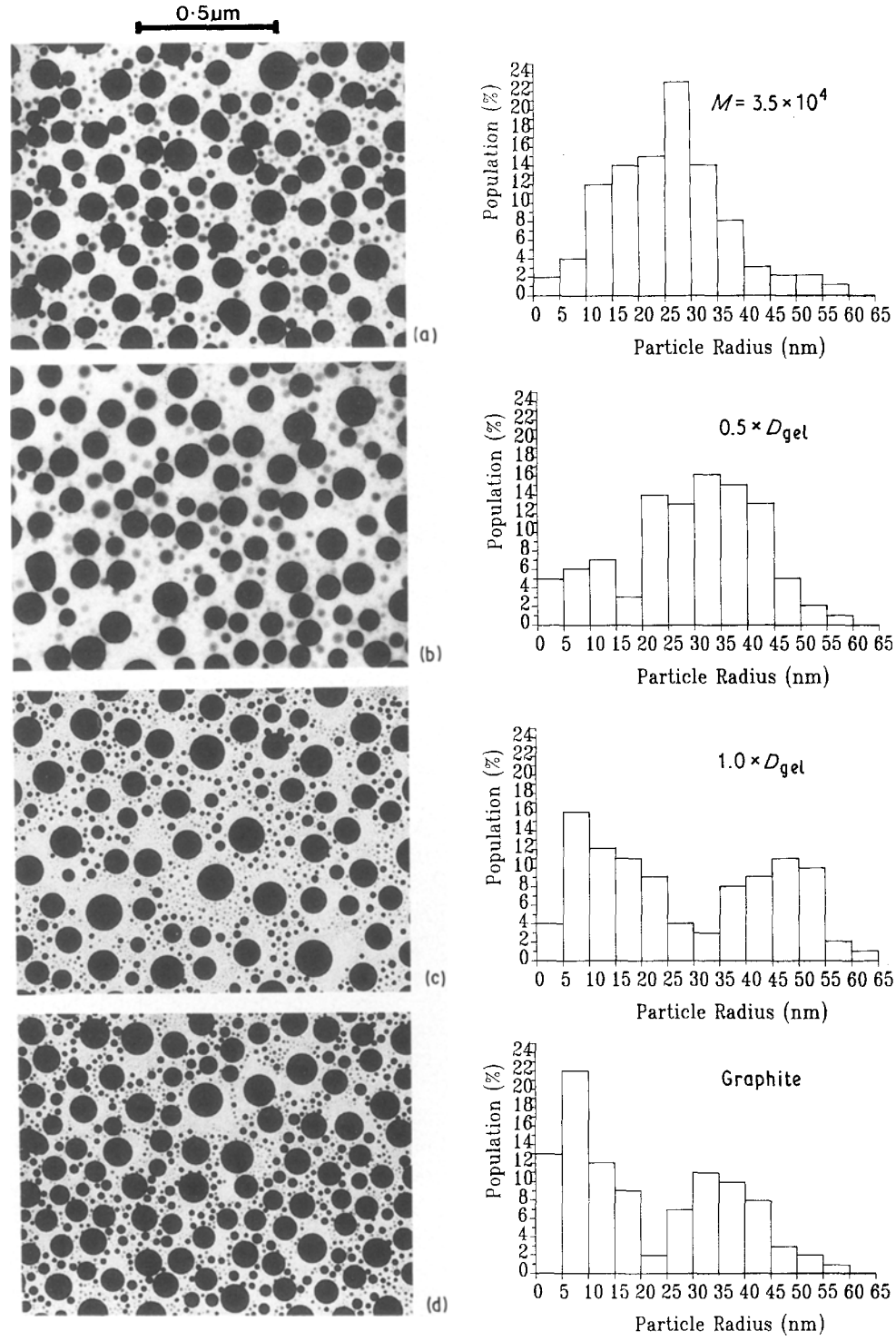

Figure 3 Series A. Plan view electron micrographs, and the particle size distributions of tin deposits formed with substrates of (a) $M = 3.5 \times 10^4$. $\bar{R}_p = 28$ nm, (b) $M = 3.5 \times 10^4$, cross-linked to $0.5 \times D_{gel}$, $\bar{R}_p = 32$ nm, (c) $M = 3.5 \times 10^4$, cross-linked to $1 \times D_{gel}$, $\bar{R}_p = 30$ nm, (d) graphite, $\bar{R}_p = 24$ nm.

685 and 40 mJ m^{-2} were used for τ_1 and τ_2, respectively, while a value of 597 mJ m^{-2} was calculated for τ_{12} using the geometric mean approximation of Fowkes [19]. The viscosities of polystyrenes over the range of molecular weights used here have been reported elsewhere [15].

Consider Fig. 4. Assuming that all the incident tin "sticks" to the PS surface, then the solid line, where $F = R$, shows how, for this series of depositions, the areal coverage of the surface has to increase with increasing molecular weight, if during the deposition an equilibrium quantity of tin on the PS surface is to be reached.

It can be seen that for $M > 5 \times 10^5$, the areal coverage would have to be greater than that corresponding to randomly packed spheres. Thus if sufficient tin is deposited on to such a PS, one would anticipate a coalescence of islands occurring on the PS surface, and hence Stage 4 of the Volmer–Weber growth mode being reached. This is turn would be reflected by the presence of a bi-modal particle size distribution.

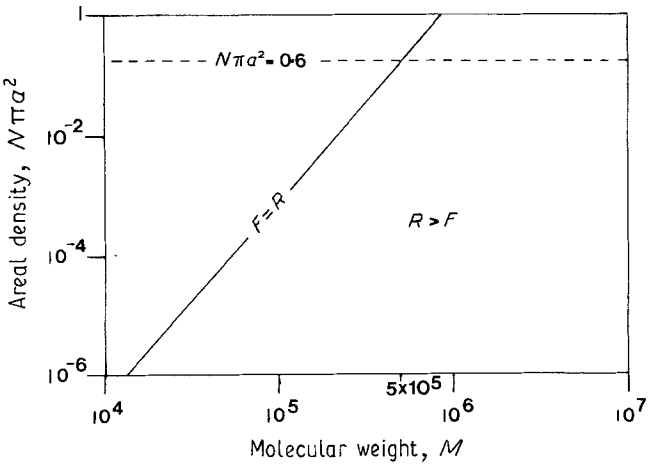

Figure 4 Modelling the kinetics of island sinking: F = flux of tin through PS surface, R = deposition flux.

Micrographs of the deposits and the corresponding particle size distributions for this series of depositions are shown in Fig. 5. Once more one sees that on increasing the molecular weight of the PS, there is an increase in the range of particle sizes. There is also an increase in the mean particle radius, presumably reflecting the increased time taken for an island to sink, during which time it can capture further adatoms, and indeed the emergence of a bi-modal distribution when $M = 1.8 \times 10^6$.

4. Conclusions

1. Growth of a sub-surface deposit of tin in softened PS occurs by a mechanism that involves the sinking of islands of tin.

2. A simple model in which the driving force for

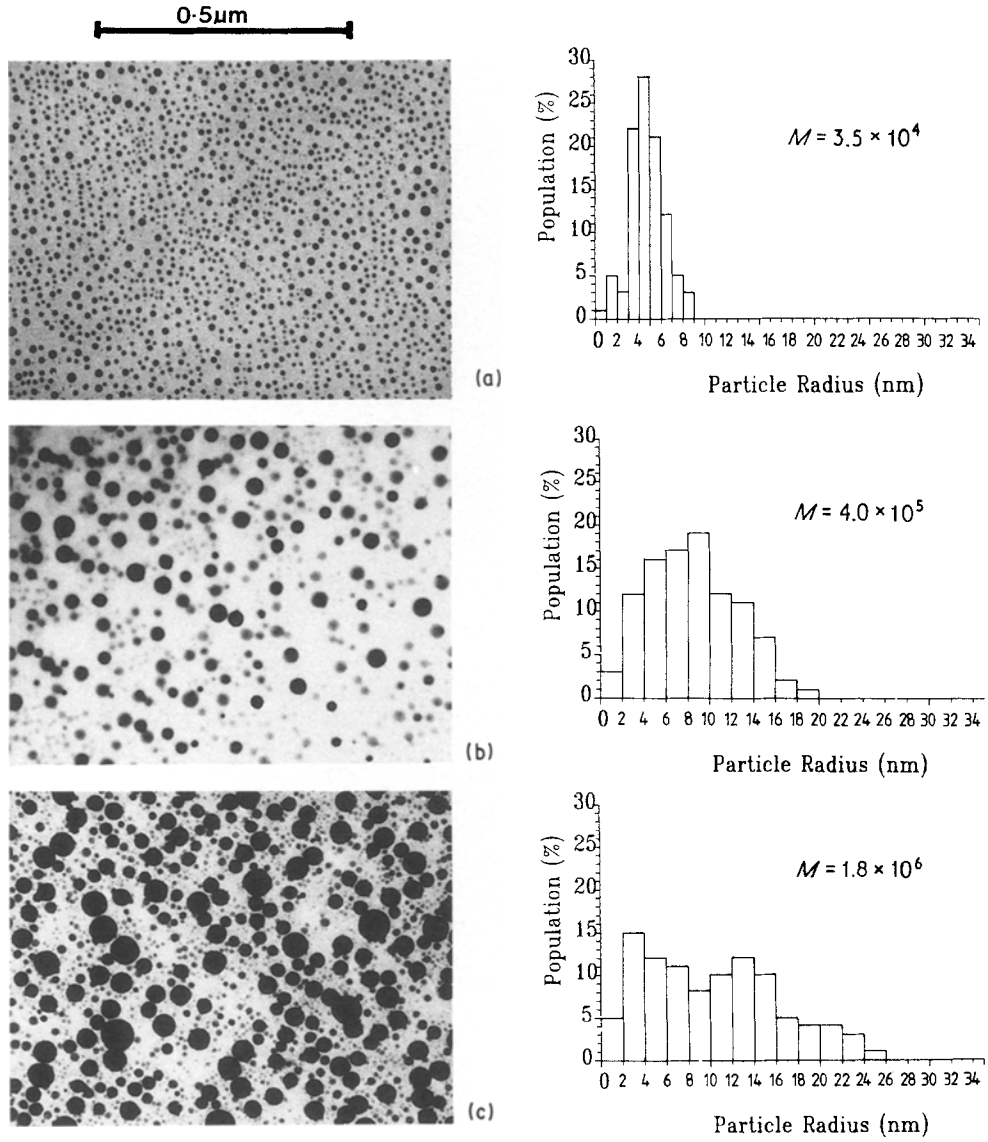

Figure 5 Series B. Plan view electron micrographs, and the particle size distribution of tin deposits formed with substrates of (a) $M = 3.5 \times 10^4$, $\bar{R}_n = 5.3$ nm, (b) $M = 4.0 \times 10^5$, $\bar{R}_n = 9.4$ nm, (c) $M = 1.8 \times 10^6$, $\bar{R}_n = 11.2$ nm.

sinking is assumed to be the reduction in surface energy of the islands, and which has sinking occurring with this force in equilibrium with the viscous drag on the islands, gives useful insight into the kinetics of the sinking.

3. The occurrence of island sinking is reflected in the particle size distribution of the deposit during the early stages of a deposition.

Acknowledgements

The authors acknowledge the financial support awarded for this work by the Research Committee of the University of Surrey. Preparation of the microtomed specimens was superbly performed by Jenny Mullervy, Microstructural Studies Unit, University of Surrey. Excellent technical support was also provided by other members of the unit.

Appendix

Assumption 1

The islands are spheres of radius a. (NB Contact angle between tin and PS is $\approx 145°$.)

The area of the cap above the surface $= 2\pi a^2 \times [1 - (a - h)/a]$ (see Fig. A1). If τ_1 = surface energy of sphere, τ_2 = surface energy of polymer and τ_{12} = interfacial energy, then the surface energy (E) of the sphere is given by

$$E = 2\pi a^2\tau_1[1 - (a - h)/a] + 2\pi a^2\tau_{12}[1 + (a - h)/a] - \pi\tau_2[a^2 - (a - h)^2] \quad \text{(A1)}$$

Assumption 2

The driving force for sinking (F_{sink}) = dE/dh. (NB The weight of the particle is only comparable when $a \approx 1500\,\mu m$.)

Therefore

$$F_{sink} = 2\pi[a(\tau_1 - \tau_{12} - \tau_2) + 2\pi\tau_2 h] \quad \text{(A2)}$$

Assumption 3

Sinking is opposed by a force (F_{surf}) which obeys Stoke's law, i.e.

$$F_{surf} = -6\pi\eta a dh/t \quad \text{(A3)}$$

where η is the viscosity of the polymer, and t the time.

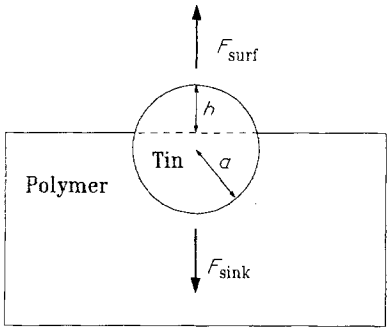

Figure A1 Model for the sinking of the islands.

Assumption 4

Sinking occurs with $F_{sink} = F_{surf}$, and that at $t = 0$, $h = 2a$, then from Equations A2 and A3 the time taken for the particle to become totally immersed (t_{im}), is given by

$$t_{im} = (3\eta a/\tau_2) \ln [\tau_1 - \tau_{12} + \tau_2)/(\tau_1 - \tau_{12} - \tau_2)] \quad \text{(A4)}$$

From which it follows that if N spheres are present per unit area the flux (F) of material through the surface is given by

$$F = (4\pi\tau_2 N a^2)/\{9\eta \ln [(\tau_1 + \tau_2 - \tau_{12})/(\tau_1 - \tau_2 - \tau_{12})]\} \quad \text{(A5)}$$

References

1. G. J. KOVACS and P. S. VINCETT, *J. Vac. Sci. Technol.* **A1(2)** (1983) 369.
2. V. N. E. ROBINSON and J. L. ROBINS, *Thin Solid Films* **20** (1975) 155.
3. J. A. VENABLES, G. D. T. SPILLER and M. HANBÜCKER, *Rep. Prog. Phys.* **47** (1984) 399.
4. G. G. STOKES, "Mathematical and Physical Papers", 2nd edn. (Johnson Reprint, New York, 1905).
5. G. J. KOVACS and P. S. VINCETT, *J. Vac. Sci. Technol.* **20** (1982) 419.
6. G. J. KOVACS, P. S. VINCETT, C. TREMBLAY and A. L. PUNDSACK, *Thin Solid Films* **101** (1983) 21.
7. G. J. KOVACS and P. S. VINCETT, *ibid.* **111** (1984) 65.
8. *Idem, ibid.* **100** (1983) 341.
9. R. M. TROMP, F. LEGOUES and P. S. HO, *J. Vac. Sci. Tech.* **A3** (1983) 782.
10. P. F. GREEN, C. J. PALMSTRÖM, J. W. MAYER and E. J. KRAMER, *Macromol.* **18** (1985) 501.
11. A. CHARLESBY and S. H. PINNER, *Proc. Roy. Soc.* **A249** (1959) 367.
12. T. E. EVERHART and P. H. HOFF, *J. Appl. Phys.* **42** (1971) 5837.
13. L. A. WALL and D. W. BROWN, *J. Phys. Chem.* **61** (1957) 129.
14. W. BURLANT, J. NEEMAN and V. SERMENT, *J. Polym. Sci.* **58** (1962) 491.
15. J. BRANDRUP and E. H. IMMERGUT, "Polymer Handbook", 2nd Edn (Wiley, New York, 1975).
16. R. A. SIGSBEE and G. M. POUND, *Adv. Coll. Interface Sci.* **1** (1967) 335.
17. D. KASHCHIEV, *Surface Sci.* **86** (1979) 14.
18. K. KINOSITA, *Thin Sol. Films* **85** (1981) 223.
19. F. M. FOWKES, *Ind. Engng Chem.* **56** (1964) 40.

Received 4 January
and accepted 17 August 1989